The Effect of Lift Position on Helicopter Recovery to a Twin-Island Aircraft Carrier

Dr Neale Watson, Professor Ieuan Owen, Professor Mark White
University of Liverpool
Liverpool, United Kingdom

Richard Lynn
QinetiQ
Farnborough, United Kingdom

ABSTRACT

This paper describes an investigation of the air flow over the flight deck of a twin-island aircraft carrier with the ship's lifts in a raised and lowered position, and the subsequent change in the aerodynamic loads on a helicopter in hover over the deck. The unsteady flow over the flight deck was simulated using Computational Fluid Dynamics for a 40 kt wind from 60° off the starboard. The turbulence intensity and velocity flow field produced over the flight deck for each lift configuration was analyzed and compared. An experimental study was conducted in which the mean and unsteady flow over a 1:200 scale model the aircraft carrier submerged in a large recirculating water channel was measured with the lifts in the raised and lowered position. The CFD prediction of the flow over the full-scale aircraft carrier was compared to the experimental velocity data. To analyze the effect of the two airwakes on a helicopter in hover, a technique known as the Virtual AirDyn was used to quantify the unsteady forces and moments acting on the aircraft. Thirty seconds of time-varying velocity data simulated for each lift configuration was integrated with a flight dynamics model of a helicopter representative of a Seahawk SH-60B. The helicopter was fixed in hover positions over the flight deck and subjected to each unsteady airwake. The resultant unsteady aerodynamic loads acting on the aircraft were analyzed to assess the effect of the lift positions on the helicopter in hover. The results show that for the conditions considered, while the lifts' positions do affect the air flow and the aerodynamic loading, there will only be a limited impact on a recovering helicopter.

INTRODUCTION

HMS Queen Elizabeth, Figure 1, is one of two new UK aircraft carriers and was commissioned in 2017. The ship has a displacement of 65,000 tonnes, with a length of 280 m and a beam of 73 m. As can be seen in Figure 1, the ship has a twin island configuration and a ramp, or 'ski-jump' at the bow. Although the carrier has been primarily designed to operate the Short Take-off and Vertical Landing (STOVL) version Lockheed Martin F-35B Lightning II, the ship will also operate with rotary-wing assets such as Merlin, Wildcat, Chinook and Apache helicopters. The recovery and launch of helicopters to and from ships at sea is regarded as one of the most demanding and dangerous environments in which a pilot may operate, particularly in strong winds (Ref. 2). The ship's motion, the availability of visual cues and the turbulent air flow caused by the ship's superstructure, known as the ship's airwake, contribute to overall pilot workload (Ref. 3). The airwake is one of the largest contributing factors to pilot workload during helicopter launch and recovery. The air flow within the airwake is typically characterized by unstable shear layers and vortices shed from the ship's superstructure and deck edges. Many of these vortices are of a similar scale to the helicopter, imparting significant fluctuating forces and moments to the aircraft, and requiring the pilot to make frequent control inputs. A number of studies have been performed to develop tools to accurately describe and simulate the ship's airwake in an effort to understand its effect on the helicopter handling qualities and pilot workload, e.g. Refs. 4, 5.

Figure 1. HMS Queen Elizabeth (© Crown copyright Ref. 1).

The unsteady air flow across the flight deck of an aircraft carrier emanates from the deck edges and from the island structures, particularly when the upstream wind is approaching from off the starboard side of the ship. Since the early days of aircraft carriers coming into service, it has been recognized that the air flow over the deck can adversely affect flying operations, and attempts have been made to suppress flow separation at the deck edges by adding passive flow control devices, e.g. Refs. 6-8. Comparable studies have been undertaken in which local modifications to a frigate's superstructure have been shown to affect the ship's airwake and, consequentially, pilot workload (Ref. 9). It is therefore understood that modifications to the ship's geometry can significantly affect the air flow and the aerodynamic loading of an aircraft when flying close to the ship. Of particular relevance to this study, aircraft carriers have lifts that are used to transfer aircraft between the flight deck and the hangar. The lifts may be raised or lowered, thereby significantly altering the geometry of the ship, as shown in Figure 2.

Figure 2. Lowered forward lift of HMS Queen Elizabeth (© Crown copyright Ref. 1).

This paper will describe a study into the effect of lift positions on the airwake of the twin-island aircraft carrier and the subsequent effect on a rotorcraft in hover above the flight deck. The aircraft carrier's airwake in a 40 kt wind approaching from 60° off the starboard side, known as a Green 60 wind, was computed for each lift configuration using time-accurate Computational Fluid Dynamics (CFD). An experimental study was also performed to measure the flow over a 1:200 scale model of the ship in a large recirculating water channel to compare with the full scale CFD prediction of the airwake. To analyze the impact of the lifts in raised and lowered positions on a helicopter in hover, the computed unsteady air velocities were integrated with a flight dynamics model of a helicopter configured to represent a SH-60B Seahawk, using a software analysis tool known as the Virtual AirDyn (VAD), which evaluates the unsteady aerodynamic loads on a stationary helicopter (Ref. 9).

SHIP AIRWAKE CFD MODELLING

The unsteady air flow over the ship, (the 'airwake'), for each lift configuration was computed using a time-accurate CFD method which has previously been used by the authors to compute the airwakes for a range of ships and validated using experimental data (Refs. 3, 4, 9, 10). Only a brief description of the CFD process and its experimental validation is included here, but a more detailed description can be found in Ref. 10.

To produce the mesh required for CFD, two geometry models, representative of the aircraft carrier, were created with the lifts in raised and lowered positions, as shown in Figure 3. Typically, when the lifts are in a raised position the hangar doors are closed; however, when the lifts are lowered the hangar doors are open. To account for any change in flow features in the simulation resulting from the open hangar doors, a simplified internal hangar cavity was also included in the geometry model of the ship with the lifts in a lowered position. The aircraft carrier model has two lifts which can be lowered independently; to reduce the number of possible computations, the lifts were modelled with both in a raised position, or both in a lowered position.

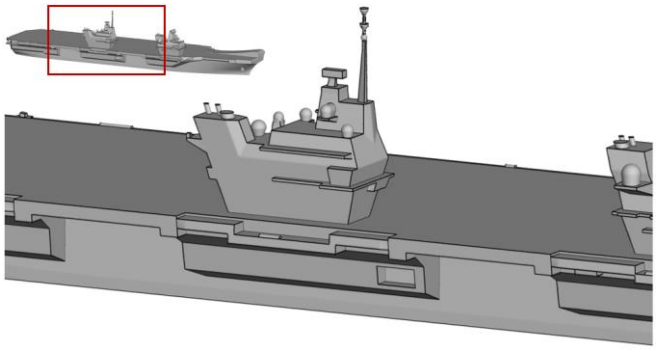

(a)

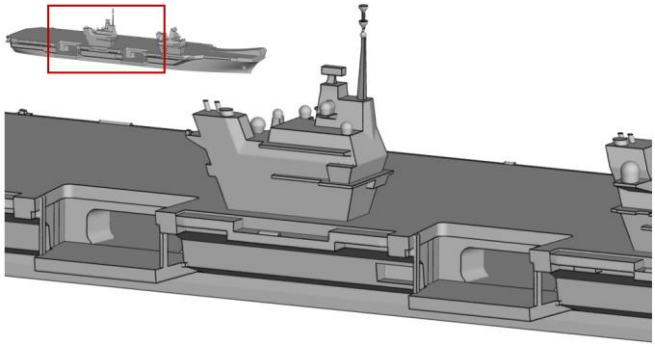

(b)

Figure 3. CAD model of a twin island aircraft carrier with a) the lifts raised and b) the lifts lowered.

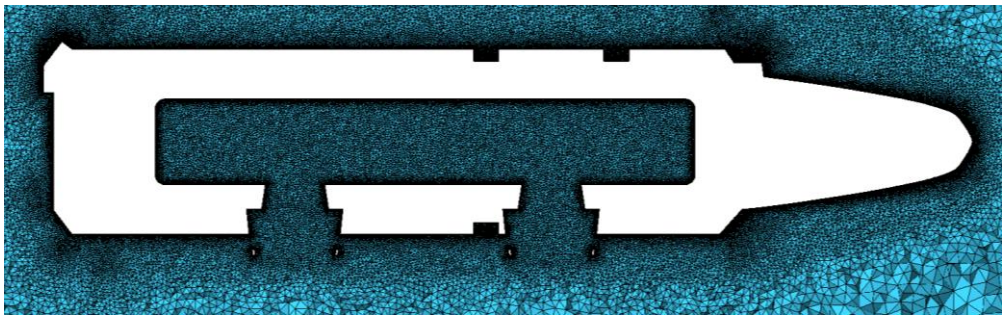

Figure 4. A horizontal plane at mid-height of the hangar through the hangar cavity showing the mesh.

Delayed Detached Eddy Simulation (DDES) was used to compute the flow over the full-scale, 280 m long ship. DDES is particularly suited to modelling unsteady flow dominated by both quasi-periodic large-scale structures and chaotic small-scale turbulent features typical of bluff body geometries (Ref. 11). DDES is a hybrid CFD method, utilizing Large Eddy Simulation (LES) to resolve large-scale structures away from the ship and Unsteady Reynolds-Averaged Navier-Stokes (URANS) to resolve the flow close to the surface (Ref. 12) using an SST k-ω based turbulence model. Momentum was solved with the third-order MUSCL discretization scheme to reduce numerical diffusion and increase spatial accuracy. DDES is well suited to ship-airwake simulations as the unsteady flows in the regions of interest over the flight deck are explicitly resolved and the computational time is reduced compared with just applying LES to solve the entire flow field, and requiring higher mesh density to resolve the flow near the ship surface. The resolution of the turbulent features using LES also reduces the dissipation of turbulent kinetic energy in the flow shed from the bluff superstructure when compared with a URANS approach. To ensure the flows in the regions of interest are explicitly resolved by LES within the DDES model, the mesh must be sufficiently dense over the flight deck, the hangar, and in the vicinity of the lifts of the ship. To resolve the turbulence over the flight deck for rotary-wing flight simulation, in which the internal flow of the hangar was accounted for, a mesh of about 50 million cells was required. Figure 4 shows a slice of the mesh in a horizontal plane located at mid-height of the hangar where the region of dense cells in the vicinity of the lifts and within the internal hangar can be seen.

The ship geometries were placed in the centre of a cylindrical domain which allows various wind directions to be modelled without the need for remeshing. A steady atmospheric boundary layer (ABL) was applied to the inlet boundary of the CFD

domain to represent the flow over the sea surface (Refs. 4, 10, 13-15). A settling period is required during the CFD computation, after which, the three-dimensional velocity components were sampled for 30 seconds to provide the unsteady airwake data to be integrated with the helicopter flight dynamics model. Figure 5 shows the full-scale aircraft carrier with the ABL velocity profile in a headwind; the plane of the image is through the centre of the islands and the unsteady airwake is illustrated by the mean normalized streamwise velocity component.

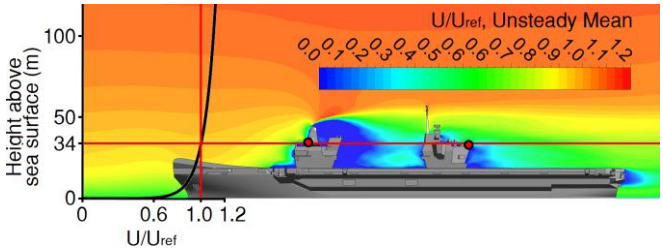

Figure 5. Atmospheric Boundary Layer.

CFD Airwake Comparison

Figure 6 shows the vortical structures in the CFD-generated flow over each ship geometry using the Q-criterion vortex identification method, colored with turbulence intensity. Overall, the air flow over the flight deck, with the lifts raised or lowered, is shown to be turbulent and likely to impact aircraft operating to the ship in a Green 60 wind. Careful scrutiny of the two images shows that when the lifts are raised, Figure 6 (a), there is a region aft of each island where there are no vortices; when the lifts are lowered, Figure 6 (b), those regions are no longer present and instead the air flow aft of the islands contains vortical structures. The reason for the difference is that the starboard deck-edge has effectively moved inboard when the lifts are down and in the oblique wind vortices are shed both from the lift platform and the 'new' deck edge.

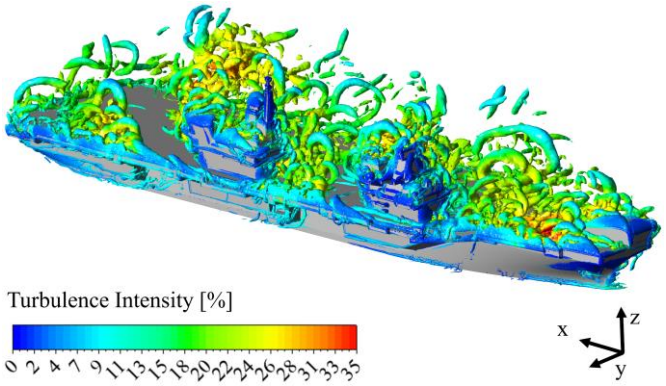

(a)

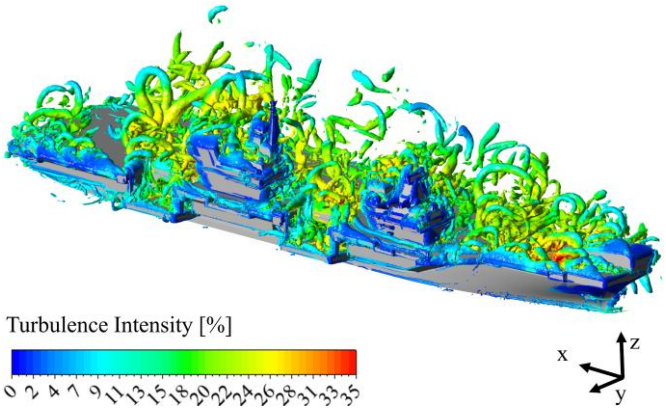

(b)

Figure 6. Green 60 flow over the aircraft carrier presented as instantaneous iso-surfaces of Q-criterion colored by turbulence intensity with the lifts (a) raised (b) lowered.

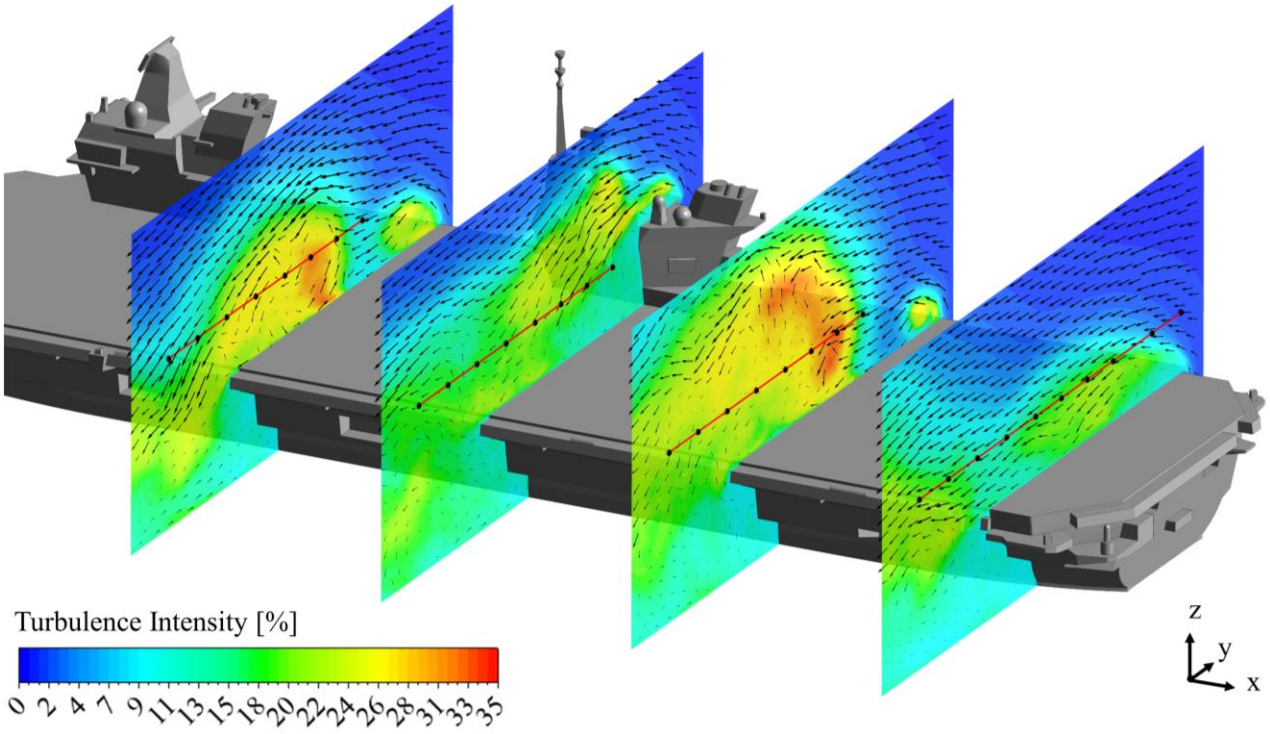

(a)

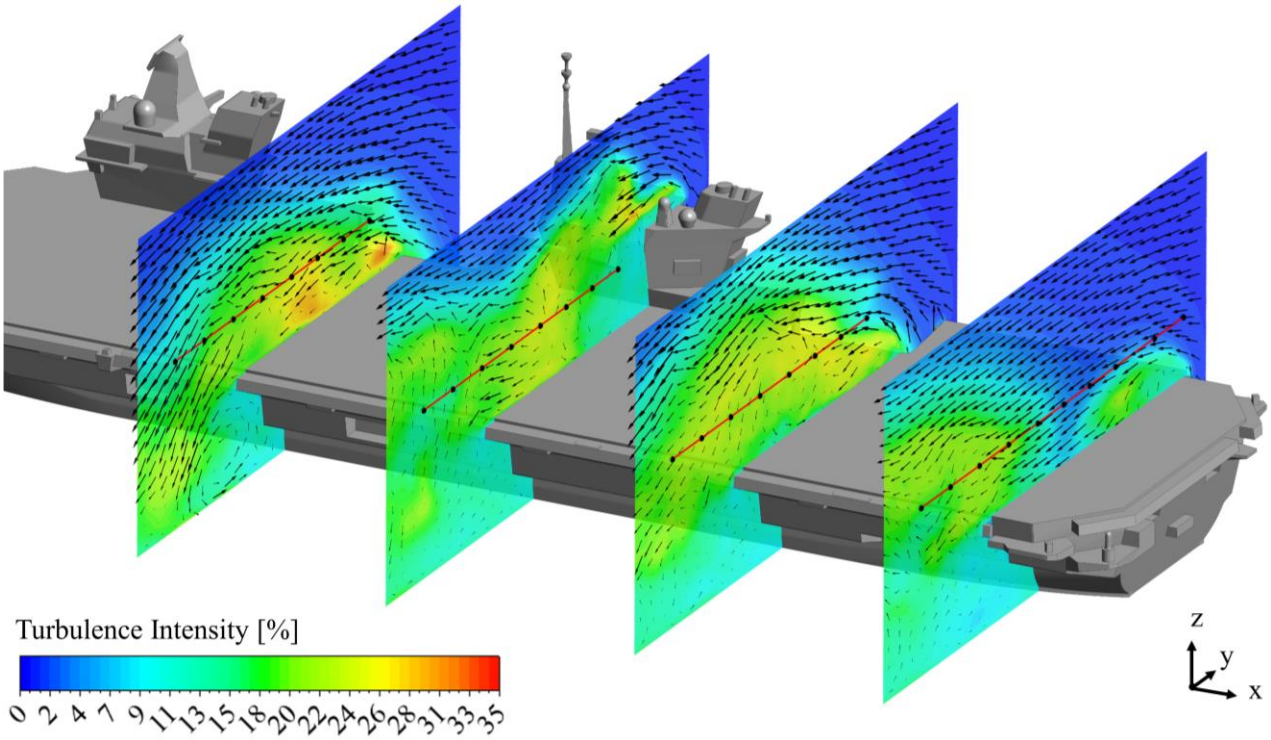

(b)

Figure 7. Velocity vectors plotted tangentially to contours of turbulence intensity with the lifts (a) raised (b) lowered.

positions along the deck of the ship, illustrated by velocity vectors and contours of turbulence intensity, for the lifts raised (a) and lowered (b). Each plane passes through a deck landing spot. The standard manoeuvre for recovering a helicopter to a UK Royal Navy ship is known as the forward-facing port-side recovery where the helicopter approaches from a position behind the ship and off the port side. The pilot stabilizes the aircraft at a distance of about one rotor diameter off the port side in line with the designated landing spot, matching the speed of the ship. The pilot then guides the aircraft sideways in a lateral manoeuvre until over the landing spot and holds position until ready to descend to the deck. The red lines in Figure 7 are 10 m above the deck and approximately represent the path of the helicopter during the lateral traverse. The black dots along each red line are where the helicopter was placed during the VAD analysis, which will be discussed later in the paper. The velocity vectors in the most forward lateral plane in Figure 7 show that the when the adjacent lift is lowered, there is a reduction in the size of the recirculation zone over the flight deck and the turbulence intensity along the lateral flight path is also reduced, compared with when the lift is raised. Similarly, comparing the velocity vectors and turbulence contours in the third vertical plane in Figure 7 (a) and (b) shows that when the lifts are lowered the turbulence intensity in the area over the flight deck adjacent to the aft lift is reduced by approximately 10%. The flow in the second plane in Figure 7, to the portside of the aft island, appears to be relatively insensitive to the positioning of the lifts in the Green 60 wind. The flow in the fourth, most aft, lateral plane also appears to be less sensitive to the positioning of the lifts although, when the lifts are lowered, the recirculation zone due to the flow separating from the starboard deck-edge is smaller.

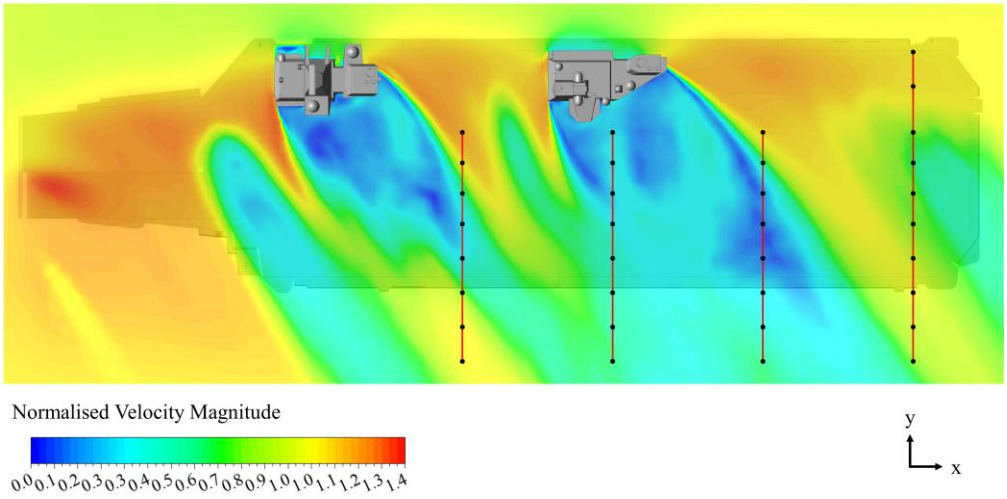

(a)

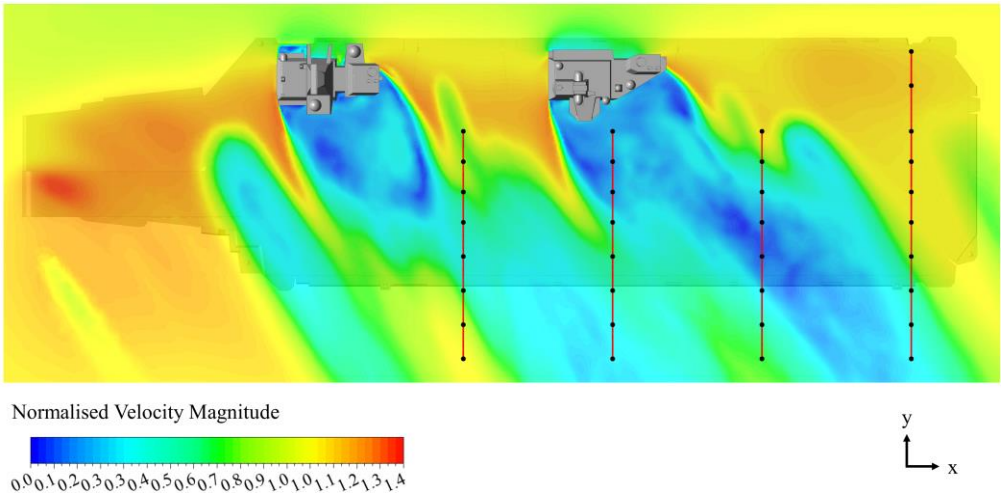

(b)

Figure 8. Mean velocity magnitude in a vertical plane 10 m above the flight deck with the lifts (a) raised (b) lowered.

Figure 9. The 3D-printed 1:200 scale experimental model of a twin-island aircraft carrier.

The velocity magnitude, normalised by the upstream reference velocity U_{ref}, in a plane located 10 m above the flight deck of the ship with the lifts raised and lowered is shown in Figure 8. It can be seen that when the lifts are lowered, Figure 8 (b), the area in which the flow accelerates through the gap between the islands has moved from aft of the forward island to forward of the aft island. Otherwise, although the mean flow field in this plane is different for the two configurations, the differences are not dramatic. From the airwake data in Figure 7 and Figure 8, while differences in the air flow can be seen, their effects on a recovering helicopter is difficult to assess from viewing the CFD alone.

EXPERIMENTAL VALIDATION

To give some confidence in the CFD method, the computed airwakes of the aircraft carrier, with the lifts raised and lowered, were compared with experimental measurements of mean velocity and turbulence over a physical model of the aircraft carrier. However, as discussed above, the airwakes were computed at full-scale, and with an ABL. The experiments were carried out in a water channel using a 1:200 scale model with a uniform inlet velocity profile. The Reynolds of the flows in each case are very high (~10^6 and 10^8) so the two flows are independent of Reynolds number and scale. As seen earlier in Figure 5, the ABL has a lower velocity close to the sea surface so the comparison between experiment and CFD is only indicative; nevertheless, the comparison was still seen as valuable.

The 1.4 m long scale-model of the aircraft carrier was manufactured from Acrylonitrile Butadiene Styrene (ABS) using 3D printing techniques and submerged in the recirculating water channel at the University of Liverpool (UoL). To withstand the oncoming flow when submerged in the water channel, slender parts such as the mast were produced using Direct Metal Laser Sintering with cobalt-chrome to achieve the required stiffness. The model was attached to the floor of the water channel using five suction cups housed within the hollow hull of the ship and connected to a vacuum pump. The ship was originally produced for a more extensive study in a previous project (Refs. 10,16).

To provide experimental measurements of the flow when the ship's lifts were lowered, and with the hangar doors open, modifications to the original 3D printed model were made allowing various model configurations to be obtained with ease during testing. Consistent with the CFD model, the physical model has an internal cavity to represent the hangar, and the doors were open when the lift was lowered, and closed when raised. The modified 3D printed model with the lifts in a lowered position with the hangar doors open is shown in Figure 9.

Experimental measurement of the flow over the submerged aircraft carrier was performed in the 90,000 litre recirculating water channel, shown schematically in Figure 10. The model was positioned on the floor of the 3.7 m long, 1.4 m wide working section of the channel with the variable floor height set to a depth of 0.85 m and the ship rotated to provide an inflow representative of a Green 60 wind. The water channel is capable of accurate inlet speeds from 1 m/s up to 6 m/s. To minimize the disturbance to the generally smooth water surface, an inlet speed of 1 m/s was applied. A brass honeycomb flow-straightener in combination with a contraction upstream of the open channel working section ensures a uniform velocity profile at the section entry, while a water jet injection at the start of the working section adds flow to the free surface to maintain the uniform velocity profile at the surface.

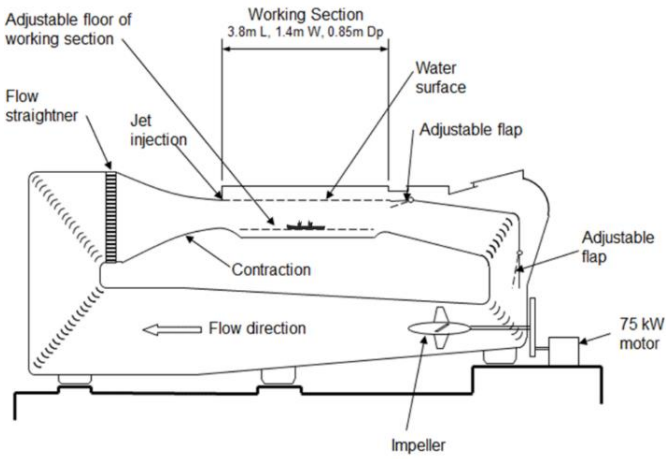

Figure 10. Schematic of water channel showing the QEC model submerged in the working section.

Mean and unsteady velocity measurements were obtained at predetermined points using Acoustic Doppler Velocimetry, ADV, a technique which detects small variations in the acoustic signal frequency arising from the Doppler effect, to measure the velocity in three components (Ref. 17). Figure 11 shows the Nortek Vectrino+ downward-facing ADV probe used in this study. The ADV probe emits a signal from the acoustic transmitter, which is then reflected to the four receivers from particles moving with the flow. The sample volume is 6 mm in diameter, 7 mm long and located 50 mm in front of the transmitter, as shown in the right of Figure 11. While mean velocity measurements may be obtained in all three components of the flow to within 1% accuracy (Refs. 17-22), turbulence may only be measured in the vertical component (the direction of the transmitter) due to Doppler noise (Ref. 19). Post-processing of the ADV output signal, necessary to remove erroneous data that affects turbulent statistics (Refs. 22, 23), was accomplished using an adaption of the "spike detection" filter in Ref. 24, first proposed in Ref. 23.

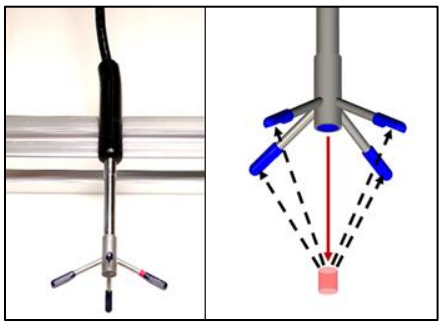

Figure 11. Nortek Vectrino+ ADV downwards-looking probe and schematic showing measurement volume relative to the probe transmitter and receivers.

To achieve positional accuracy and repeatability of each measurement within the water channel, the ADV probe was attached to a three-dimensional motorized programmable traverse providing positional accuracy of 0.1 mm. The model aircraft carrier was positioned in the flume within 2 mm of positional accuracy in the *x*, *y* and *z* directions (cartesian axes are illustrated in the various CFD images). However, using the in-built distance tool of the ADV probe, the sample volume could be positioned within 1 mm of the ship's surface in the *x*, *y* and *z* directions, thereby providing a positional accuracy of about 1.1 mm. Velocity data measured at the same points in an area of unsteady flow at varying times during the day, and on consecutive days, were found to be within 1% which confirms the repeatability of the measurements. At each point in the flow, the velocity components were measured over a period of 60 seconds at a sample rate of 200 Hz giving a total of 12,000 individual raw samples per velocity time history.

Figure 12 and Figure 13 show comparisons between the computed and experimentally measured flow over the ship with the lifts raised, and with the lifts lowered and hangar doors opened. Measurements were taken along all four lines shown in Figure 7 and Figure 8; however, data is only presented for the third line i.e. adjacent the aft lift and 10 m above the deck, where the flow differences are most pronounced.

Figure 12 shows the mean velocities in three components and the vertical turbulence intensity, computed using CFD and measured by ADV, with the lifts in a raised position. Bearing in mind the different inlet conditions, there is good agreement between CFD and ADV of the *u* and *w* velocity components in Figure 12; there is less agreement in *v* but the overall trend

across the flight deck is predicted. The measured vertical turbulence intensity also agrees well with the CFD, with the exception of the point on the centerline of the ship; however, this point is at the edge of the shear layer where flow features are sensitive to position within the flow.

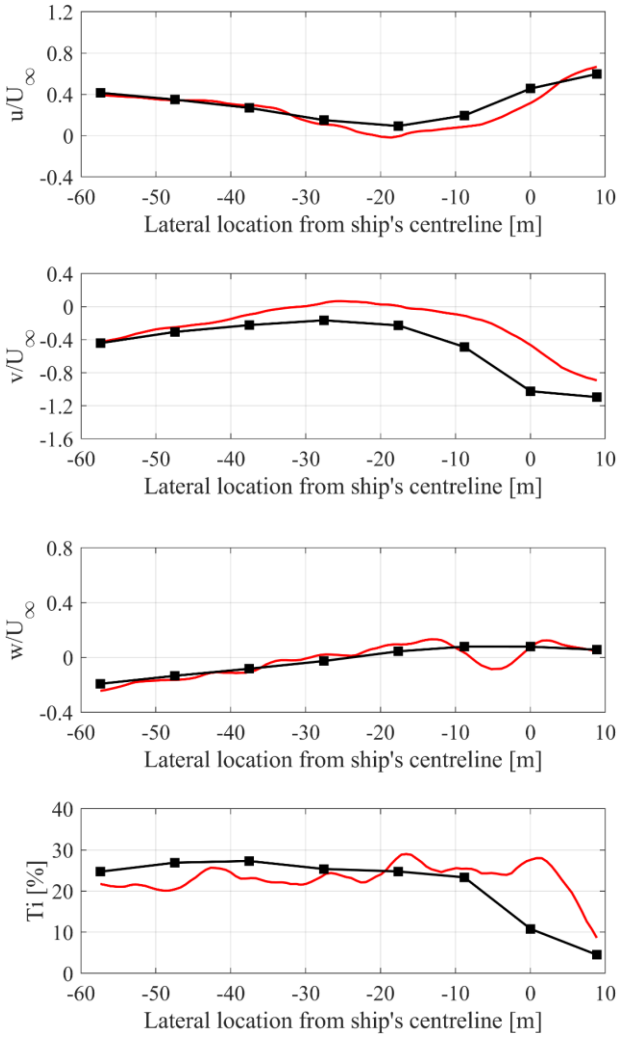

Figure 12. CFD-ADV comparison with the lifts raised.

A comparison of the flow generated using CFD and measured by ADV with the lifts in a lowered position, and the hangar doors open, is shown in Figure 13; each measurement point is at the same location as in Figure 12. Again, there is good agreement between the numerical and experimental *u* and *w* velocity components in Figure 13. The CFD-generated *v* velocity is predicted to be slightly higher between -30 m and -15 m from the ship's centerline; however, the profile follows the same trend as the ADV measurement. The vertical turbulence intensity again shows good agreement between CFD and ADV, with a similar exception as shown in Figure 12 where there is a disagreement in the turbulence intensity at the sample point on the centerline of the ship.

In general, there is good agreement between the CFD-generated airwake and the experimental measurements, for both lift configurations, despite the differences in scale and inlet velocity profile. The agreement between experimental and numerical solutions provides confidence in the CFD method for the unsteady velocities in the airwake to be applied to a helicopter flight dynamics model in the VAD analysis.

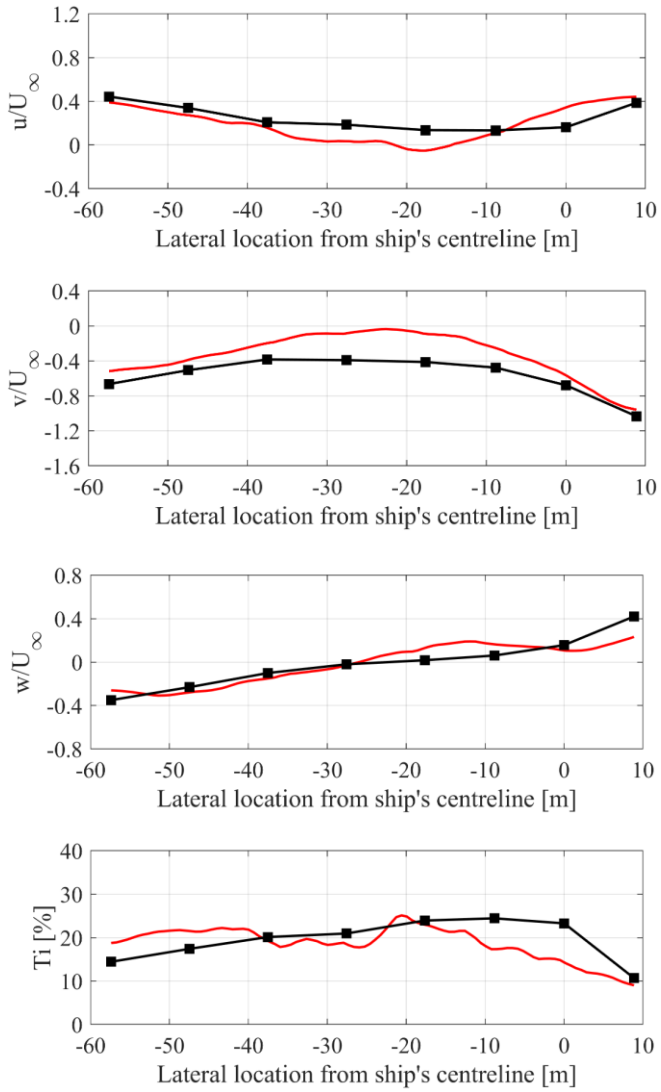

Figure 13. CFD-ADV comparison with the lifts lowered.

AIRWAKE INTEGRATION

For the helicopter to be subjected to the ship's airwake within the VAD, the 30 seconds of unsteady velocity components generated by CFD are imposed on the aircraft flight dynamics model at various locations on the rotor blades and airframe within FLIGHTLAB (Ref. 25), a commercial software package which provides a multi-body modelling and simulation environment. Figure 14 shows a schematic of how the CFD-generated data is processed. The raw unstructured CFD data is first interpolated onto a grid of 1 m spacing in the area of interest over the flight deck. The raw CFD data was generated at 100 Hz; however, to reduce the amount of data stored, and to allow real-time playback, the interpolated data was down-sampled to 25 Hz. The bottom left of Figure 14 shows the boundary of the interpolated airwake, which encompasses the majority of the flight deck from the forward island to off the stern of the ship, as well as areas extended off the flight deck where aircraft may be approaching the ship. The interpolated airwake is then converted into a series of look-up tables within Simulink which are fed into the FLIGHTLAB model of a helicopter representative of a Seahawk SH-60B. The airwake velocities are applied in real-time via 46 Aerodynamic Computation Points (ACPs) shown in Figure 14 as red dots, ten of which are located along each main rotor blade; the remaining points are positioned at the aircraft's center of gravity (c.g.), the vertical tail, the tail rotor hub and the starboard and port stabilizers. While the airwake velocities are read by the aircraft flight dynamics model, the aircraft's downwash is not included and fed back to the airwake model, resulting in what is known as a one-way coupled simulation.

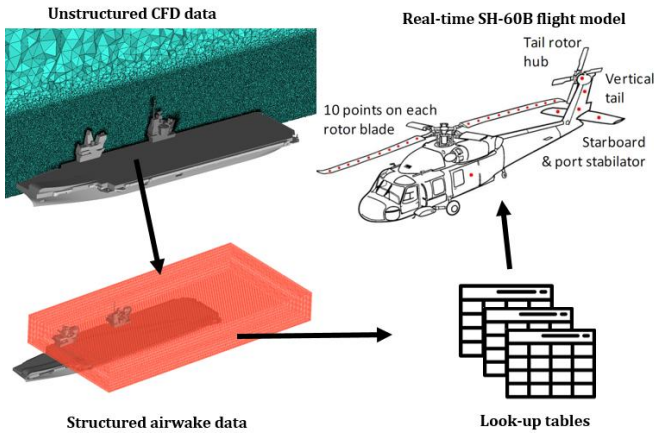

Figure 14. Integration of CFD airwake with helicopter flight dynamics model.

THE VIRTUAL AIRDYN

While the CFD results have provided views of the unsteady flow field over the flight deck and have highlighted areas of steep velocity gradients, it is difficult to assess how these will affect the helicopter. The VAD technique is used to calculate the unsteady aerodynamic loads imposed onto a helicopter by the unsteady air flow.

The VAD is a software analysis tool which quantifies the impact of the airwake on a helicopter by integrating the unsteady velocity components with a helicopter flight dynamics model (Ref. 9). During piloted real-time simulations, the unsteady velocities in the airwake will produce time-varying forces and moments through the helicopter's flight dynamics model that will cause the aircraft to deviate from the trim condition, requiring the pilot to compensate for these disturbances through helicopter control inputs. In the VAD, the helicopter model is placed in the prevailing freestream condition and trimmed before being placed at a selected point in the airwake and fixed in that position. When the unsteady airwake velocities are applied to the helicopter in the fixed position it will experience time-varying non-zero forces and moments. The forces and moments on the helicopter are recorded by the VAD over the 30-second period of the airwake and provide a quantitative measure of the aerodynamic loads, calculated at the helicopter's c.g. Previous research at UoL has employed the VAD to investigate the effect of ship airwakes on helicopter handling qualities and pilot workload (Ref. 9, 26) and for evaluating and comparing different ship design modifications (Ref. 27).

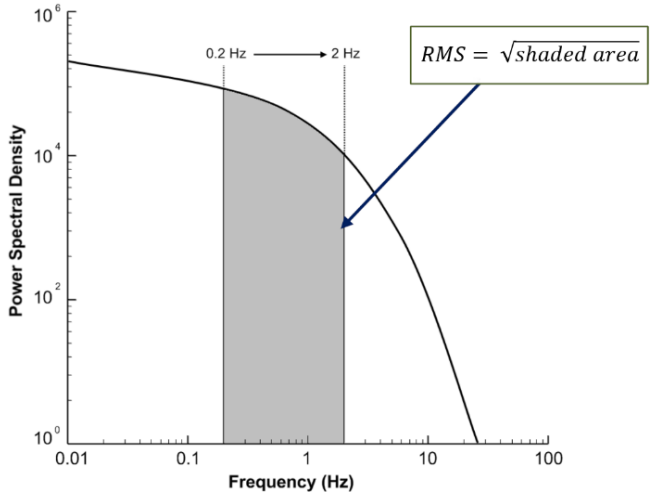

Figure 15. Method for calculating RMS forces and moments acting on helicopter flight dynamics model.

The VAD was placed at the points along the third lateral line shown in Figure 7 and Figure 8, adjacent to the aft lift; i.e. the same line as the CFD/experiment comparison in Figure 12 and Figure 13. The points correspond to the helicopter's rotor hub. The helicopter model was subjected to 30 seconds of airwake for each lift configuration. The resulting forces and moments acting on the aircraft were recorded and show unsteady loads created over a wide range of frequencies. However, it is loads in

the range 0.2 to 2 Hz which are the main contributors to pilot workload (Ref. 28), known as the pilot closed-loop response frequency range. At frequencies much below this range, disturbances will be 'quasi-steady' and manifest themselves as a drift which, if not corrected by the pilot, will result in large aircraft displacements. Frequencies above 2 Hz are experienced as vibrations through the airframe that will mainly impact ride quality.

To analyze the effect of the time-varying airwake on the aircraft, the resultant unsteady forces and moments on the helicopter, simulated by the VAD, are filtered to only include the frequencies associated with pilot workload. At each location, the root mean square (RMS) value in the unsteady forces (thrust, side, drag) and moments (roll, pitch, yaw) are computed over the pilot's closed-loop response frequency range of 0.2 to 2 Hz by calculating the Power Spectral Density (PSD) plot of each time history and calculating the square root of the integral between the upper and lower bounds, as shown schematically in Figure 15.

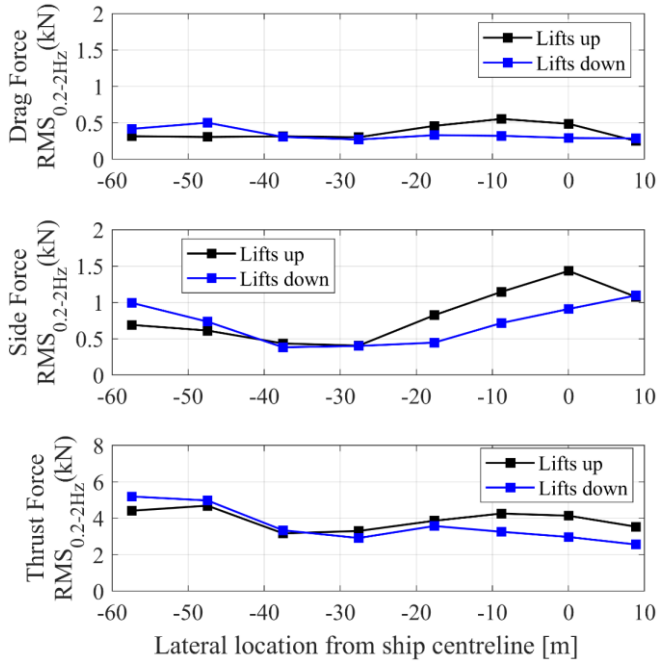

Figure 16. VAD RMS forces acting on the aircraft fixed in hover.

Figure 16 shows the VAD RMS forces acting on the aircraft fixed in hover along the lateral line adjacent to the aft lift for the two lift configurations. Every RMS force is higher with the lifts in a raised position at hover locations between -20 m and 0 m from the ship's centerline, which is consistent with the higher turbulence intensity observed in Figure 7, and the helicopter's proximity to the shear layer shedding off the aft island shown in Figure 8. At the two hover locations between -40 m and -20 m, the RMS forces are similar and suggest that the position of the lifts has little effect on the helicopter at these hover positions. Figure 7 shows a slight increase in turbulence intensity at these two points; however, as the mean flow velocity is low, as shown in Figure 8, the change in turbulence appears to have little effect on the rotorcraft. An increase in each force RMS is observed at the two most portside hover positions when the lifts are in a lowered position. While the turbulence intensity at these points is similar, the mean velocity is higher, thereby indicating a higher velocity fluctuation.

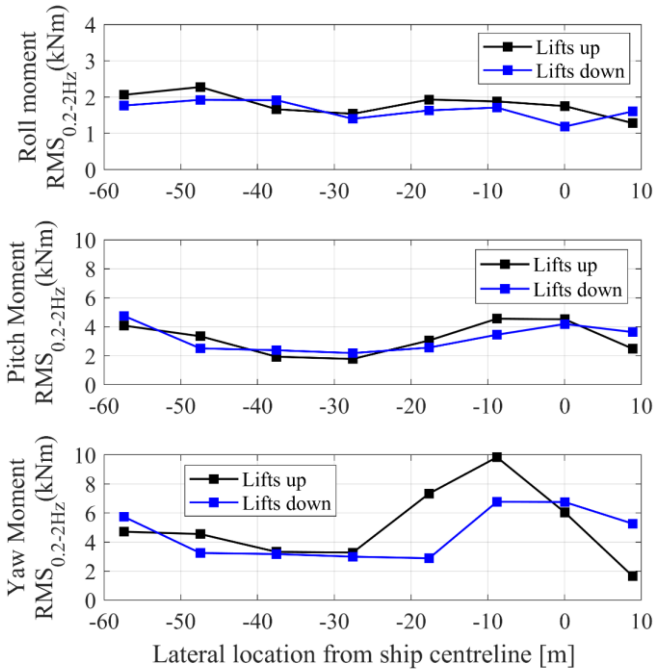

Figure 17. VAD RMS moments acting on the aircraft fixed in hover.

Figure 17 shows the corresponding VAD RMS moments acting on the helicopter fixed in hover along the same lateral line. While the majority of the VAD locations shows the rolling moment RMS is reduced slightly when the lifts are in a down position, the values are similar. The pitching moment RMS in Figure 17 also shows that the RMS values are similar whether the lifts are raised or in a lowered position. The lowest pitching moment RMS values are observed for each lift configuration at the two points between -40 m and -20 m, which corresponds to areas of both low turbulence intensity, and low mean velocity magnitude as shown in Figure 7 and Figure 8. The yaw moment RMS shows relatively larger differences with the lift raised and lowered in the area of the shear layer from the aft island. At the point closest to the lift, the airwake generated with the lifts in a lowered position creates a larger yaw moment RMS, which, may be due in part to the effect of the tail rotor positioned in the wake of the aft island, as shown in Figure 8; at the same location when the lifts are raised, the tail rotor will be in freestream air. At the two hover points between -20 m and -5 m, the yaw moment RMS is much higher when the lifts are raised. Figure 8 suggests this is due to the aircraft is operating within or close to a strong shear layer. Hover points to the portside of the ship (less than -20 m laterally) show that the lifts lowered has a similar effect on the yaw moment RMS as the lifts raised.

CONCLUSIONS

This paper has described an investigation into the effect of the lift positions of a twin-island aircraft carrier on the airwake over the flight deck, and its subsequent effect on a helicopter in hover. Time-accurate CFD was used to simulate the unsteady airflow over the ship in a wind approaching from 60° off the starboard with both lifts in a raised and a lowered position; the flow within the internal hangar cavity was also simulated when the lifts were lowered. Thirty seconds of unsteady CFD has been used to calculate the mean and turbulent velocities over the flight deck and the flow field for each lift configuration was compared. To provide confidence in the CFD method and solution, the mean and unsteady flow over a representative 1:200 scale model of the ship submerged in a water channel was measured using Acoustic Doppler Velocimetry. The flow over the ship in the water channel was measured at various locations to capture both the three mean components of velocity and the vertical turbulent statistics to compare with the numerically computed flow. The time-varying airflow created by CFD was integrated with a helicopter flight dynamics model of a SH-60B Seahawk helicopter. Using a technique known as the Virtual AirDyn, which quantifies the unsteady forces and moments acting on the aircraft in the hover, the effect of the ship airwakes, with lifts in a raised and lowered position, on a helicopter in hover was therefore assessed.

The main conclusions can be listed as follows:

i. Winds approaching a twin-island aircraft carrier from 60° off the starboard side will create significant turbulent air flow over the flight deck in the wake of the ship's superstructure.

ii. Lowering the lifts and opening the hangar doors will create changes in the flow field over the flight deck of a twin island aircraft carrier. Turbulence intensity in regions over the flight deck of the aircraft carrier is reduced when the lifts are in the lowered position. The lifts in a lowered position extend the low velocity wake region emanating from the aft island of the aircraft carrier.

iii. ADV experimental measurements of mean and turbulent velocities over the flight deck of the model ship showed generally good agreement with the CFD solutions of each lift configuration, and provided confidence in use of the CFD generated airwake for flight simulation.

iv. The airwake generated with the lifts in a raised position produces larger force fluctuations on a helicopter close to the lift. Further away from the lift the force fluctuations are similar up to a point portside of the ship where the force fluctuations are larger with the lifts in a lowered position.

v. The rolling and pitching moment fluctuations on the helicopter in hover are similar for each lift configuration; however, at hover locations close to the lift, the yaw moment fluctuations differ, perhaps due to the varying position of shear layer produced by each airwake.

vi. Overall, the analysis has shown that having the lifts in a raised or lowered position will have limited effect on a recovering helicopter. However, there are some differences and a helicopter in hover close to the aft lift will experience a greater impact from the airwake when the lifts are raised. Further to the portside of the deck, the impact will be similar for each lift position. Off the portside edge of the ship, the lifts in a lowered position will create higher fluctuations in the forces on the helicopter.

Author contact: Neale Watson nawatson@liv.ac.uk

ACKNOWLEDGMENTS

The authors acknowledge the ongoing support form ANSYS U.K., Ltd. The experimental program was carried out under contract to QinetiQ. The authors acknowledge the support of QinetiQ in developing the experimental program. The authors would also like to thank John Curran at the University of Liverpool for his work and expertise in modifying the original 3D printed model of the aircraft carrier and Glen Friel for his technical support in the water tunnel facility.

REFERENCES

1. Royal Navy Imagery Database, accessed March 2020 https://www.royalnavy.mod.uk/useful-resources-and-information/rn-image-archive

2. Lumsden, B., and Padfield, G. D., "Challenges at the helicopter-ship dynamic interface," 24th European Rotorcraft Forum, Marseilles, France, September 1998.

3. Roper, D., Owen, I., Padfield, G. D. and Hodge, S. J. "Integrating CFD and piloted simulation to quantify ship-helicopter operating limits," *The Aeronautical Journal*, 2006, Vol. 110 (1109), pp. 419-428. https://doi.org/10.1017/S0001924000001329

4. Owen. I., White, M. D., Padfield, G. D., and Hodge, S. J., "A virtual engineering approach to the ship-helicopter dynamic interface – a decade of modelling and simulation research at the University of Liverpool," *The Aeronautical Journal*, 2017, Vol. 121 (1246), pp. 1833-1857. https://doi.org/10.1017/aer.2017.102

5. S. Shukla, S. S. Sinha, and S. N. Singh, "Ship-helo coupled airwake aerodynamics: A comprehensive review," *Progress in Aerospace Sciences*, 2019, Vol. 106 (1), pp. 71-107. https://doi.org/10.1016/j.paerosci.2019.02.002

6. Nangia, R. K., and Lumsden, R. B., "Novel vortex flow devices – columnar vortex generators studies for airwakes," Proceedings of the 34th AIAA fluid dynamics and exhibition, Portland, OR, 28 June–1 July 2004, AIAA paper 2004-2348. https://doi.org/10.2514/6.2004-2348

7. Czerwiec, R. M., and Polsky, S.A., "LHA airwake wind tunnel and CFD comparison with and without bow flap,", Proceedings of the 22nd AIAA applied aerodynamics conference and exhibition, Providence, RI, 16–19 August 2004, AIAA paper 2004–4832.
https://doi.org/10.2514/6.2004-4832

8. Bardera-Mora, R., Barcala-Montejano, M.A., Rodrıguez-Sevillano, A. and Nova-Trigueros, J., "Passive flow control over the ski-jump of aircraft carriers", *Ocean Engineering*, 2016, Vol. 114, pp. 134–141.
https://doi.org/10.1016/j.oceaneng.2016.01.019

9. Kääriä, C. H., Forrest, J. S. and Owen, I., "The Virtual AirDyn: a simulation technique for evaluating the aerodynamic impact of ship superstructures on helicopter operations," *The Aeronautical Journal*, 2013, Vol. 117 (1198), pp. 1233-1248.
https://doi.org/10.1017/S0001924000008836

10. Watson, N. A., Kelly, M. F., Owen, I., Hodge, S. J. and White, M. D. "Computational and experimental modelling study of the unsteady airflow over the aircraft carrier HMS Queen Elizabeth," *Ocean Engineering*, Vol. 172, 2019, pp. 562-574.
https://doi.org/10.1016/j.oceaneng.2018.12.024

11. Spalart, P. R., Deck, S., Shur, M. L., Squires, K. D., Strelets, M. Kh. and Travin, A. "A New Version of Detached-Eddy Simulation, Resistant to Ambiguous Grid Densities," *Theoretical and Computational Fluid Dynamics*, 2006, Vol. 20 (3), pp. 181-195.
https://doi.org/10.1007/s00162-006-0015-0

12. Spalart, P. R., "Comments on the feasibility of LES for wing and on a hybrid RANS/LES approach," 1st ASOSR Conference on DNS/LES, Arlington, TX, August 1997.

13. Forrest, J. S and Owen, I., "An Investigation of Ship Airwakes Using Detached-Eddy Simulation," *Computers & Fluids*, 2010, 39 (4), pp. 656–673.
https://doi.org/10.1016/j.compfluid.2009.11.002

14. Garratt, R., *The Atmospheric Boundary Layer*, Cambridge Atmospheric and Space Science Series, Cambridge University Press, 1992.

15. Watson, N. A., Owen, I., and White, M. D., "Piloted Flight Simulation of Helicopter Recovery to the Queen Elizabeth Class Aircraft Carrier," *Journal of Aircraft*, Vol. 57 (4), Jul 2020, pp. 742-760.
https://doi.org/10.2514/1.C035733

16. Watson, N. A., Owen, I., and White, M. D., "Experimental Validation of the Unsteady CFD-generated Airwake of the HMS Queen Elizabeth Aircraft Carrier," AIAA Aviation Forum, Dallas, USA, 17-21 June, 2019. AIAA paper 2019-3029.
https://doi.org/10.2514/6.2019-3029

17. Kraus, N. C., Lohrmann, A., and Cabrera, R., "New Acoustic Meter for Measuring 3d Laboratory Flows," *Journal of Hydraulic Engineering*, Vol. 120 (3), March 1994, pp. 406-412.
https://doi.org/10.1061/(ASCE)0733-9429(1994)120:3(406)

18. Lane, S. N., Biron, P. M., Bradbrook, K. F., Butler, J. B., "Three-dimensional measurements of river channel topography and flow processes using acoustic Doppler velocimetry," *Earth Surface Processes & Landforms*, Vol. 23, (13), December 1998, pp. 1247-1267.
https://doi.org/10.1002/(SICI)1096-9837(199812)23:13<1247::AID-ESP930>3.0.CO;2-D

19. Voulgaris, G., and Trowbridge, J. H., "Evaluation of the Acoustic Doppler Velocimeter (ADV) for Turbulence Measurements," *Journal of Atmospheric and Oceanic Technology*, Vol. 15 (1), February 1998, pp. 272-289.
https://doi.org/10.1175/1520-0426(1998)015<0272:EOTADV>2.0.CO;2

20. Lohrmann, A., Cabrera, R., and Kraus, N., "Acoustic-Doppler Velocimeter (ADV) for Laboratory Use," Fundamentals and Advancements in Hydraulic Measurements and Experimentation, American Society of Civil Engineers, Buffalo, New York, August 1994.

21. Lopez, F., and Garcia, M. H., "Mean flow and turbulence structure of open-channel flow through nonemergent vegetation," *Journal of Hydraulic Engineering*, Vol. 127, (5), May 2001, pp. 392–402.

https://doi.org/10.1061/(ASCE)0733-9429(2001)127:5(392)

22. Chanson, H., Trevethan, M. & Aoki, S., "Acoustic Doppler velocimetry (ADV) in small estuary: Field experience and signal post-processing," *Journal of Flow Measurement and Instrumentation*, Vol 19, 2008, pp. 307-313. https://doi.org/10.1016/j.flowmeasinst.2008.03.003

23. Goring, D. G. & Nikora, V. I., "Despiking Acoustic Doppler Velocimeter Data," *Journal of Hydraulic Engineering*, Vol 128 (1), 2002, pp. 117–126. https://doi.org/10.1061/(ASCE)0733-9429(2002)128:1(117)

24. Wahl, T. L., "Discussion of 'Despiking acoustic Doppler Velocimeter data' by Derek G. Goring and Vladimir I. Nikora," *Journal of Hydraulic Engineering*, Vol 129 (6), 2003, pp. 484–488. 10.1061/(ASCE)0733-9429(2003)129:6(484)

25. Du Val, R. W. and He, C, "Validation of the FLIGHTLAB virtual engineering toolset," *The Aeronautical Journal*, Vol 122 (1250), April 2018, pp. 519-555. https://doi.org/10.1017/aer.2018.12

26. Watson, N. A., Kelly, M. F., Owen, I., and White, M. D., "The Aerodynamic Effect Of An Oblique Wind On Helicopter Recovery To The Queen Elizabeth Class Aircraft Carrier," Vertical Flight Society's 75th Annual Forum, Philadelphia, PA, USA, May 13-16, 2019.

27. Forrest, J. S., Kääriä, C. H. and Owen, I., "Evaluating ship superstructure aerodynamics for maritime helicopter operations through CFD and flight simulation," *The Aeronautical Journal*, 2016, Vol. 120 (1232), pp. 1578-1603. https://doi.org/10.1017/aer.2016.76

28. McRuer, D. T., "Interdisciplinary interactions and dynamic systems integration," *International Journal of Control*, Vol. 59 (1), 1994, pp. 3-12. https://doi.org/10.1080/00207179408923067